A high-resolution titrator: a new approach to studying binding sites of microbial biosorbents

Ghinwa Naja[a], Christian Mustin[b], Bohumil Volesky[a],*, Jacques Berthelin[b]

[a]*Department of Chemical Engineering, McGill University, 3610 University Street, Montreal, Que., Canada H3A 2B2*
[b]*LIMOS, UHP Nancy 1, Faculté des Sciences, Domaine Victor Grignard, B.P. 239, F 54506, Vandoeuvre les Nancy, France*

Abstract

The high-resolution potentiometric titration was used as a physico-chemical method to study the acid properties of selected biosorbent materials in order to quantify the functional acidic groups for sorption and to determine their affinities by considering their partial or total ionization equilibrium reactions. The Gran's method and the Henderson–Hasselbach's equation were employed in establishing the partition of the total acidity as associated with strong, weak and very weak acidic chemical active groups. The differences in the total organic acidity (A_{TO}) for the two selected types of bacteria and two mycelia revealed by this method were explained by the chemical composition of their cell walls. The total organic acidities obtained were $3.87 \, \mathrm{me \, g^{-1}}$ for *Thiobacillus ferrooxidans*, $1.31 \, \mathrm{me \, g^{-1}}$ for *Corynebacterium glutamicum*, $0.81 \, \mathrm{me \, g^{-1}}$ for *Aspergillus niger* and $2.54 \, \mathrm{me \, g^{-1}}$ for *Rhizopus arrhizus*.

The links between the activity of protons and the sorption capacities of the selected bioorganic matters were established. Sorption of lead by *C. glutamicum* and *R. arrhizus* biomass indicated an optimum pH of 6. It appeared that 64% ($\mathrm{Pb_{(uptake)}} = 0.48 \, \mathrm{me \, g^{-1}}$) and 38% ($\mathrm{Pb_{(uptake)}} = 0.28 \, \mathrm{me \, g^{-1}}$) of A_{TO} were involved during lead sorption onto *R. arrhizus* and *C. glutamicum*, respectively.

The applications of titration techniques become a powerful tool for the characterization of heterogeneous materials involved in biosorption and bioremediation processes.
© 2004 Elsevier Ltd. All rights reserved.

Keywords: Gran's method; High-resolution potentiometric titration; Acidic functional groups; Sorption capacity

1. Introduction

Sorption is an important physico-chemical process which greatly affects the fate and mobility of ions in soil and water (McBride, 1994; Sposito, 1984; Stumm, 1992). Biosorption could occur through interactions between metal ions and functional groups of the cell wall biopolymers of living and dead organisms (Beveridge, 1986; Daughney et al., 2001; Gadd, 1988; Sing and Yu, 1998; Volesky et al., 1993; Yee and Fein, 2001). The physico-chemical properties of these constituents, such as the nature of the functional groups and the specific surface area, are involved in reactions such as biosorption, bioleaching and flocculation exploited in many industrial applications (Volesky, 2003). However, chemical mechanisms responsible for biosorption of metal ions by organic matter, chemically and structurally heterogeneous, are poorly understood. It has been suggested (Fourest et al., 1994; Schiewer and Volesky, 1997) that specific functional groups are involved in the

*Corresponding author. Tel.: +1 514 398 4276;
fax +1 514 398 6678.

E-mail address: boya.volesky@mcgill.ca (B. Volesky).

biomass binding process of heavy metals (Sarret et al., 1998). During sorption reactions, cations compete with protons for these complexing sites.

The organic matter used in the present study, fungi and bacteria, contains polysaccharides, proteins and lipids and can be considered as polyelectrolyte with amino, carboxyl, phosphate and sulfate groups. The diversity of the functional groups and their polyelectrolyte nature call for the application of the acid–base potentiometric titration method, concepts and theory. This approach has also been previously used to study the formation of soluble organo-metallic complexes (Brunelot et al., 1989). The proton or hydroxyl are considered as indicators allowing description of the energetic distribution of the surface sites.

The acid–base titration can help to: (1) estimate the cationic exchange capacities of biosorbents (Coleman et al., 1959); (2) identify the acid ionizable functional groups or binding sites which can play the role of ligand in the presence of protons or others toxic metal ions (Pagnanelli et al., 2004), and (3) describe the chemical heterogenic reactivity of the organic surface (Cox et al., 1999). This approach can yield valuable specific data for further quantitative sorption work.

This work is aimed at studying the reactivity of functional groups in heterogeneous organic matter, dead fungi and bacteria. It attempts to quantify the functional acidic groups and to describe organic cell wall reactivity estimated by considering partial or total ionization equilibrium reactions using a high-resolution acid–base potentiometric titration (HRT) based on Gran's method (Gran, 1952; Rossotti and Rossotti, 1965) and on Henderson–Hasselbalch equations estimating the equivalence volumes and the affinity distributions. The knowledge of this functional chemical distribution could be employed to explain the more probable mechanism of metal immobilization on the cell wall.

1.1. Background

Potentiometric titrations such as the type used in this work determine the end point (i.e. the inflection point) of the classical S-shape titration curves. The result is a plot of volume of the titrant added versus the potential of the electrode, giving direct information about the concentration in solution, using the Nernst equation:

$$E = E_0 + RT/nF \log \{H^+\}, \tag{1}$$

where E_0 and E are the standardization potential and the potential measured by the electrode (V), respectively, R the gas constant ($8.3144\,J\,mol^{-1}\,K^{-1}$), T the temperature (K), n the number of the exchanged electrons, F the Faraday constant ($96487\,C\,eq^{-1}$) and $\{H^+\}$ the protons activity in solution.

The inflection point of the curve pH = f(Volume) provides the end point and consequently the equivalence volume. While for many applications this method is suitable, in the case of the titration of heterogeneous organic matter, this approach often leads to unsatisfactory results:

- the inflection point is obscured partially by the buffering action of water or by the "undulation" of the titration curve. The determination of the inflection point becomes very difficult;
- the asymmetry of the curve may invalidate the assumptions that the inflection point corresponds exactly to the end point. Furthermore, the accuracy of a titration is generally limited by the correct and reproducible detection of the equivalence point.

One way to solve this problem is to use the derivative functions and then searching for zero values of the second derivative (Kucharkowski et al., 1984). However, for heterogeneous matter titrations, the derivative curve may be sometimes complicated to interpret and the determination of the inflection point becomes subjective. The application of Gran's method to heterogeneous organic matters, as presented in this study, allows determining precisely the equivalence volume and the distribution of total acidities.

2. Materials and methods

2.1. Biosorbent materials

The types of bioorganic matter used to verify the titration accuracy were:

- two fungal species *Aspergillus niger* DSM 821 and *Rhizopus arrhizus* DSM 905, cultivated in a liquid medium at 24 °C in the dark (Roux et al., 1988). After 5–6 days of growth, fungal biomass was collected by filtration, washed, dried and ground;
- acidophilic Gram-negative bacteria *Thiobacillus ferrooxidans* DSM 583, cultivated in a batch reactor (30 °C) containing ferrous sulfate at pH = 1.8 (Temple and Colmer, 1951). After 3 days of growth, biomass was collected by filtration and centrifugation (Beckman J2-21; 15,000*g* for 20 min);
- Gram-positive bacterial strain *Corynebacterium glutamicum* provided by a food industry.

All samples were washed several times with distilled water to eliminate culture medium residues and lyophilized.

2.2. Acid–base titrations

All high-resolution titration experiments were conducted in a 100 ml, jacketed glass vessel (Wheaton) sealed by a lid fitted with four ports for a titrant injection, a N_2 line, a pH electrode and a temperature probe, respectively. The vessel temperature was maintained at 25 °C by recirculation of thermostated water from a bath through the vessel jacket. The headspace was purged with N_2 at low pressure during titration to remove CO_2. Titrant aliquots of a specified volume (down to 1 µl) were injected through a polypropylene line by an automatic and accurate burette (ABU901 Radiometer). The solution in the vessel was agitated by a magnetic stirrer (500 rpm) until pH became stable after each titrant aliquot injection. All experiments were carried out with 0.1 M $NaClO_4$ solution as the background electrolyte. pH was measured using a Ross combined electrode (Ross 8102) and a pH meter (PHM250 Radiometer). The inner KCl electrode solution was replaced by a saturated NaCl solution to avoid $KClO_4$ precipitation in the electrode liquid junction. For basic titration, the titrant used was 0.026 M NaOH solution with a low content of carbonates. Before each biomass titration, a calibration was performed with the background electrolyte, sodium perchlorite, previously acidified to pH 2.3 with 0.056 N $HClO_4$ then aliquots of NaOH were added until pH 10.5 is reached.

The minimum quantity of biomass required for reliable measurement was estimated to be 2 g l^{-1}. This was based on obtaining a minimum volume difference of 1.2 ml between the acid volume V_a and the base volume V_b in the Gran's plots, and not to exceed 0.35 ml in the control, an acceptable maximum difference attributed to the atmospheric CO_2.

Especially developed original automated high-resolution titration control system (PC, TestPoint Software) allowed the release of variable volumes into the potentiometric titration cell, according to proportional conditions. This multitasking and interactive system permitted to change the different operating parameters during the experiments such as the volume, rate and frequency of injections, and the stability factor considering the complex nature of different solids to be titrated. The stability factor took into account the derivatives at the previous six equilibrium points. Each equilibrium point was attained when a potential difference less than 0.2 mV was observed during 10 min.

2.3. FTIR analysis

To complete the study of the functional groups, an IR analysis was performed with a Fourier Transform Infrared (FTIR) spectrometer (Brüker Vector 22). Each 1 mg dried sample (24 h P_2O_5) was mixed with 200 mg of KBr (Spectranal) and pressed under vacuum. The tablet recovered with a clip, was immediately analyzed with a spectrophotometer in the range of 4000–400 cm^{-1} with a resolution of 1 cm^{-1}. The influence of atmospheric water and CO_2 were always subtracted.

2.4. Sorption experiments

Finally, sorption experiments were conducted using stirred, thermostated (25 °C) batch reactors to analyze sorption capacities of R. arrhizus, representing fungi and C. glutamicum, representing bacteria (1 g l^{-1}). The initial concentration of $Pb(NO_3)_2$ was 100 mg l^{-1} at pH 4, 5 and 6. After 24 h of equilibration time, the solution was filtered (0.45 µm) to remove the biomass and the concentration of lead remaining in solution was measured by inductively coupled plasma—atomic emission spectrometry (ICP-AES, Jobin Yvon JY 238).

The amount of complexed metal was calculated by difference between the initial and equilibrium solution concentrations.

3. Theoretical considerations

3.1. Gran's method

In 1952, Gran (Gran, 1952; Rossotti and Rossotti, 1965) presented a mathematical technique for converting a conventional S shaped titration curve into two straight lines that intersect at the end point. To apply this method to a heterogeneous matter, the sorption surface is regarded as a succession and a continuous distribution of acid sites, and the overall reactions used during an acid–base titration of a multi-polymeric acid are considered. Gran's formula follows from the definition of the acid constant K_a that can be written:

$$H_m A \Leftrightarrow mH^+ + A^{m-}, \qquad (2)$$

$$K_a = \frac{[H^+]^m [A^{m-}]}{[H_m A]} \qquad (3)$$

with

$$[H_m A] = \frac{A_0 V_0 - N_0 V}{V_0 + V} = \frac{N_0 (V_e - V)}{V_0 + V}, \qquad (4)$$

$$[A^{m-}] = \frac{N_0 V}{V_0 + V}, \qquad (5)$$

and

$$\{H^+\} = 10^{-pH} = f_{H^+}[H^+], \qquad (6)$$

where V_0 is the initial volume (ml), V the titrant added volume (ml) and V_e the equivalence volume (ml) being the volume of base added when the equivalence point is

reached. N_0 is the normality of the base used and A_0 the acid concentration of the initial solution.

The definition of the Gran function is as follows:

$$G = (V_0 + V)10^{(k_1 - \text{pH})} = k_2(V_e - V) \quad \text{at pH} < 7, \quad (7)$$

$$G = (V_0 + V)10^{(k_3 - \text{pH})} = k_4(V - V_e) \quad \text{at pH} > 7, \quad (8)$$

where G is the Gran function and k_1, k_2, k_3, k_4 are constants.

Supposing that a heterogeneous surface exhibits its acidities continuously as a function of the affinity constant (K_a) (de Wit et al., 1993), then the titration curves can be adjusted using symmetric Gaussian distribution functions and the total organic acidity (A_{TO}) of a sample can be divided into three different chemical acidic groups depending on their apparent ionization constants:

- *strong acidities* (A_S): Evaluated from the difference between the volume of NaOH added ($V_a - V_{aN}$) and can be attributed to the presence of high affinity acidities, such as phosphoric or sulfonate groups, as well as carboxylic groups linked to aromatic functions at pH < 4;
- *weak acidities* (A_W): Considered from the volume ($V_e - V_a$), are attributed to the ionization of carboxylic and some proteic groups at 4 < pH < 7; and
- *very weak acidities* (A_{VW}): Calculated from the volume ($V_b - V_e$), are attributed to phenolic and amine groups including the ionization of amino groups of proteins at pH > 7.

The evaluation of these acidities follow from the different equations:

$$A_S (\text{me} \, l^{-1}) = \frac{(V_a - V_{aN})}{V_0} \times N_0, \quad (9)$$

$$A_W (\text{me} \, l^{-1}) = \frac{(V_e - V_a) - (V_{eN} - V_{aN})}{V_0} \times N_0, \quad (10)$$

To transform the obtained values from $\text{me} \, l^{-1}$ to $\text{me} \, g^{-1}$, the correction factor (V_0/m) is introduced where m is the mass of the biomass solids (g).

3.2. Dissociation coefficients α of weak and very weak acidities

Comparing the two titrations, of the control (electrolyte) and of the sample (electrolyte + sample), at *the same pH*, the following equation can be deduced:

$[H^+]$ control $= [H^+]$ electrolyte $+ [H^+]$ sample

$$\frac{A_0 V_{0N}}{(V_N + V_{0N})} - \frac{N_0 V_N}{(V_N + V_{0N})}$$
$$= \frac{A_0 V_0}{(V + V_0)} - \frac{N_0 V}{(V + V_0)} + A_{TO} \alpha \frac{V_0}{(V + V_0)}, \quad (12)$$

$$\Rightarrow \alpha = \frac{(A_0 + N_0)(V_{0N} V - V_0 V_N)}{V_0 (V_N + V_{0N}) A_{TO}}. \quad (13)$$

The dissociation coefficients α of the weak and very weak acidities are given by:

$$\alpha(A_W) = \frac{(A_W)_t}{(A_W)} = \frac{1}{A_W} \left\{ \frac{(A_0 + N_0)(V_{0N} V - V_0 V_N)}{V_0 (V_N + V_{0N})} - A_S \right\}, \quad (14)$$

$$\alpha(A_{VW}) = \frac{(A_{VW})_t}{(A_{VW})} = \frac{1}{A_{VW}}$$
$$\times \left\{ \frac{(A_0 + N_0)(V_{0N} V - V_0 V_N)}{V_0 (V_N + V_{0N})} - A_S - A_W \right\} \quad (15)$$

To determine the different pK_a values, the Henderson–Hasselbach equation was used to relate the dissociation sites coefficients α and the pK_a value to the pH as follows:

$$pK_a = \text{pH} + m \log \frac{1 - \alpha}{\alpha}. \quad (16)$$

$$A_{VW} (\text{me} \, l^{-1}) = \frac{[(V_b - V_e) - (V_{bN} - V_{eN})][(V - V_b) - (V_N - V_{bN})]}{V_0} \times N_0 \quad (11)$$

with $A_{TO} = A_{VW} + A_W + A_S$. The suffix N corresponds to the control.

Where V_{0N} and V_0 are the initial volume of the control and sample, respectively, V_N and V are the total volume of the base added after titration of the control and sample, respectively. V_a and V_b are volumes determined by the acidic and basic slopes, respectively, of the Gran's function representation of the sample. In the particular case of a control, $V_{eN} \approx V_{aN} \approx V_{bN}$.

The pK_a values of weak and very weak acidities, defined as the apparent constants, are derived from the pH value when $\alpha = 0.5$.

4. Results and discussion

4.1. Gran analysis of biomass titrations

Gran analysis applied to a heterogeneous matter offers several advantages:

- the use of several points to define the equivalence volume (when $G = 0$) as opposed to the inflection point, which reduces random error and increases the precision;
- the validation of the linearity of the electrode within the studied pH range, $NaClO_4$ control curve;
- two independent Gran functions, before and after the endpoint, increase the statistical reliability of the analysis;
- the partitioning of the total acidity into strong, weak and very weak acidities.

Fig. 1 gives a general idea of the Gran's function shape during a base titration of a heterogeneous matter and a control sample. The shape of the Gran curves depended on the studied material. The representation of the Gran's control function is constituted by two straight lines intersecting at V_{eN}. The Gran's function for organic matter is shifted, compared to the control, and has a curved shape when reaching the x-axis. The determination of the equivalence volume V_e of the sample is based on the zero value for the curve of the second derivative $\partial^2 pH/\partial V^2$ illustrated in Fig. 1. The shift between the control and the sample Gran curves corresponds to different kinds of acidities. The following volumes can be noted:

- V_{eN} and V_e, corresponding to the equivalence volumes of the control and the sample experiments, respectively, determined from the zero values of the function $\partial^2 pH/\partial V^2$ (sample) and of $G = f(V)$ (control);

- V_a and V_b determined by the acidic and basic slopes of the Gran's function representation of the sample. In the particular case of a control, $V_{eN} \approx V_{aN} \approx V_{bN}$ and 0.35 ml is an acceptable maximum difference between these values attributed to atmospheric CO_2.

Having the volume values V_e, V_{eN}, V_a and V_b, strong, weak and very weak acidities could be calculated following Eqs. (9)–(11). The dissociation coefficients α could be calculated from Eqs. (14) and (15).

4.2. Biomass binding sites

4.2.1. Titration curves and distribution of acidities
The total organic acidity (A_{TO}) determinations at the final titration pH value 10.5 allowed characterizing and differentiating organic matter with respect to the composition of their functional groups.

The titration curves obtained (Figs. 2 and 3) permitted to analyze the progressive dissociation of the protonated sites, to determine the A_{TO} (at pH = 10.5) of the functional groups, the quantity of the three types of acidity (A_S, A_W and A_{VW}) (Table 1) and their pK_a values (Fig. 4).

The distribution of the acidities of the two types of bacterial biomass is presented in Table 1. The values of the $A_{VW} + A_W$ exceeded 50% of the A_{TO} due to the presence of protein moieties. The A_W (20–30% of the A_{TO}) was attributed to carboxylic sites of phospholipid groups.

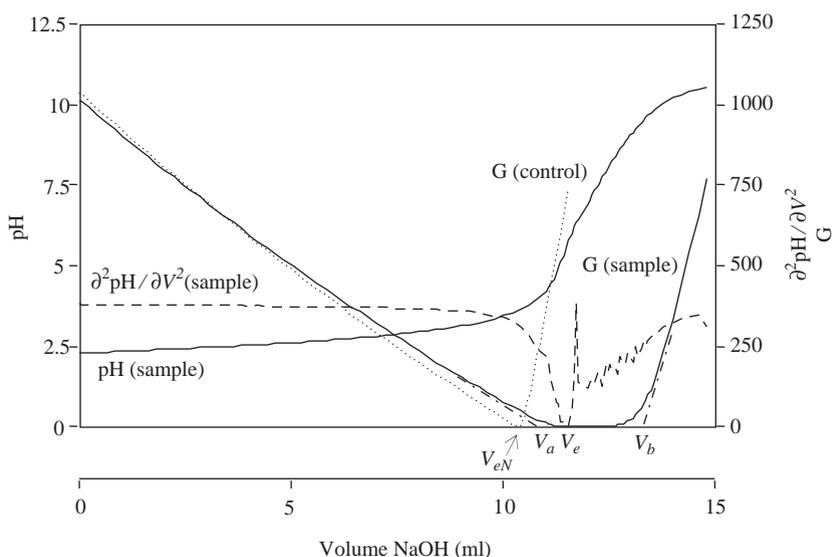The A_{TO} values obtained agreed with values derived from the same titration technique reported in the

Fig. 1. Gran's function (G), second derivative ($\partial^2 pH/\partial V^2$) and titration curves of a sample. Gran's (G) function of the control. V_{eN} and V_e correspond to the equivalence volumes of the control and the sample experiments, respectively. V_a and V_b are the acid and basic equivalence volumes of the sample determined by the acidic and basic slopes of the Gran's function.
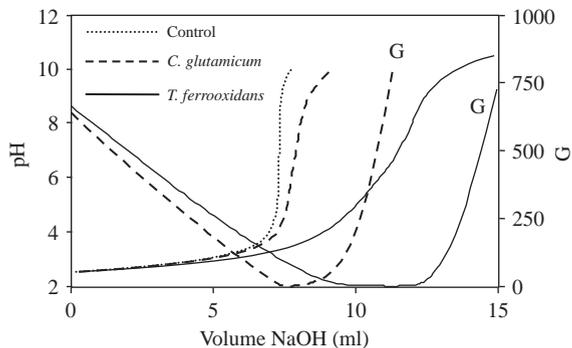
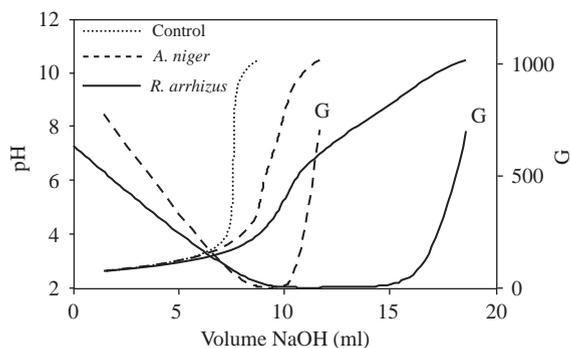Fig. 2. Titration and Gran's function G curves of the two bacteria $T.$ $ferrooxidans$ and $C.$ $glutamicum$.

Fig. 3. Titration and Gran's function G curves of the two fungi $R.$ $arrhizus$ and $A.$ $niger$.

Fig. 4. Henderson and Hasselbach's representation of bacteria ($T.$ $ferrooxidans$ and $C.$ $glutamicum$) and fungi ($R.$ $arrhizus$ and $A.$ $niger$). The symbol α represents the dissociation sites parameters.

literature for biomass of other bacteria. Pagnanelli et al. (2004) studied $Sphaerotilus$ $natans$ Gram-negative bacterium and identified a total organic acidity value of 3.2 me g^{-1}, close to $T.$ $ferrooxidans$ total organic acidity obtained in the present work. Texier et al. (2000) analyzed $Pseudomonas$ $aeruginosa$ and identified a total organic acidity value of 1.1 me g^{-1}, close to $C.$ $glutamicum$ total organic acidity obtained in the present work.

The differences in A_{TO} for the two bacteria, 3.87 me g^{-1} for $T.$ $ferrooxidans$ and 1.31 me g^{-1} for $C.$ $glutamicum$, are mainly explained by the chemical composition of their cell walls.

Gram-negative $T.$ $ferrooxidans$ bacterial cell walls have a multilayered and a chemically complex composition consisting of protein, lipopolysaccharides and peptidoglycan. Cell walls of the Gram-positive $C.$ $glutamicum$ feature a simpler single-type of a molecule. Correspondingly, they contain a lower number of active functional groups. This difference in the cell wall chemical composition influenced the sorption capacities of the two types of biosorbents. The Gram-negative bacteria, containing much higher number of active sites, can be considered as a potential alternative adsorbent
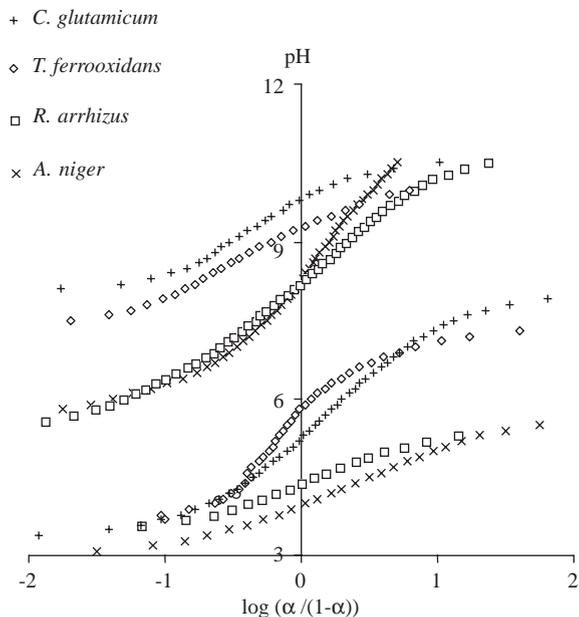
for heavy metal from aqueous solutions (Mukai et al., 2000; Pagnanelli et al., 2004).

The pK_a values (Fig. 4) of $T.$ $ferrooxidans$ and $C.$ $glutamicum$ were similar for A_W (5.3–5.8), corresponding to COOH groups. The pK_a of the A_{VW} for these biosorbents varied between 9.3 and 9.8 due to the high protein content of bacterial cell walls. Furthermore, $T.$ $ferrooxidans$ gave values for $A_{VW} \approx A_W + A_S$, indicating that its biomass has a low total charge, approaching zero, within a large pH range between 4 and 8. In this pH range, the charge developed by the weak and strong acidities is counter-balanced by the charge developed by the very weak acidities. Moreover, these bacteria have a positive charge in acid solution (pH < 3) when all the A_{VW} and A_W sites are protonated and the A_S sites are dissociated. A low bacterial surface charge between pH 4 and 8 would be favorable for their adhesion onto mineral surfaces as it limits electrostatic repulsion and decreases the activation energy necessary to establish contact between bacteria and minerals.

Knowledge of the cation exchange capacity of bacteria is important for specification of the functional groups involved in the adhesion phenomena, of the nature of the bond between the metal and the cell wall, and for establishing the optimum pH value for adhesion.

The difference between the two mycelia revealed by this method can be explained by their taxonomic classification, Ascomycetes for $A.$ $niger$ and Zygomycetes for $R.$ $arrhizus$. $A.$ $niger$ had a lower A_{TO}

Table 1
Types and amounts of acidity (me g^{-1}) and their characteristics (pK_a) for mycelia (A. niger and R. arrhizus) and bacteria (T. ferrooxidans and C. glutamicum)

	A_{TO} (me g^{-1})	A_S (me g^{-1})	A_W (me g^{-1})	pK_{a_1}	A_{VW} (me g^{-1})	pK_{a_2}
A. niger	0.81	0.005	0.35	4.0	0.45	8.3
R. arrhizus	2.54	0.27	0.39	4.4	1.88	8.2
T. ferrooxidans	3.87	0.50	1.16	5.8	2.21	9.3
C. glutamicum	1.31	0.177	0.827	5.3	0.31	9.8

A_{TO}, A_S, A_W and A_{VW} represent total organic, strong, weak and very weak acidities expressed for pH 10.5, respectively.

(0.81 me g^{-1}) than R. arrhizus (2.54 me g^{-1}). This was due to lower A_S corresponding to phosphoric or sulfonate groups, and lower A_{VW} attributed to amine groups. R. arrhizus contains more amine groups as its cell wall is mainly composed of chitin consisting of linear chains of acetylglucosamine groups conferring a global positive or neutral charge to the structure. However, the two mycelia had a similar quantity of A_W corresponding mainly to carboxylic groups (≈ 0.3 me g^{-1}).

Despite these differences, the pK_a values determined using the Henderson and Hasselbach representation (Fig. 4), were quite similar. The pK_a values for A_W (4–4.4) were mainly attributed to carboxyl groups and the pK_a values of A_{VW} (8.2–8.3) corresponded to amine and not to phenol groups which are characterized by higher pK_a values > 10.

Quantitative estimations of the total organic acidities of fungal biomass reported in the literature, divided just into strong and weak acidities, are commonly based on the first derivative curve originating from potentiometric basic titrations. Fourest and Volesky (1996) studied Sargassum fluitans biomass and by using a base titration determined the total organic acidity value of 2.20 meq g^{-1}. This value is close to the R. arrhizus total organic acidity obtained in the present work (2.54 me g^{-1}).

Although the different classes of microbial materials used in this work may contain identical acidic groups, the dissociation of the same kind of acidic functionality extends over a wide range of pH indicating that they are not present in a similar chemical configuration so as to undergo simultaneous dissociation during a base titration. This dissimilarity of the acidities distributions among the fungal and bacterial biomass types used could be explained and mainly depends on:

(a) the number of ionization sites; their types: phosphoric, sulfonate, carboxylic, amine or phenolic; their nature: the functional group can be linked to the surface through aliphatic or aromatic groups; and

(b) the gradual build up of a negative charge structure during titration leading to sites reconfigurations.

(a) *Nature and types of functional groups:* Similarities were observed when comparing the pK_a values obtained in the present work to those reported in the literature related to macromolecules extracted from soils (Young et al., 1981). The pK_a values of their carboxylic groups were between 2.5 and 5.2. The pK_a of 2.5 corresponds to a carboxylic moiety linked to an aromatic group. The pK_a of 5.2 is attributed to a carboxylic moiety linked to an aliphatic chain. The proximity of another carboxylic group could be responsible for a higher ionization and lower pK_a values. The pK_a values obtained in the present work (Table 1) indicated that the carboxylic acidic groups in the biomass types examined were linked to aliphatic chains rather than to aromatic groups.

The phenolic acidic groups have ionization constants between 9.9 and 10.8 (Martell and Smith, 1974) depending on the different substitutions of the phenolic groups. The amine ionization constants pK_a of the proteins or polypeptides fall between 8.1 and 9.6, values corresponding to those obtained in the present study (Table 1).

(b) *Charge density and configuration changes:* Biomass titration with a base leads to an increase in the number of dissociated functional groups and the build up of a negative charge which may restrict electrostatically further dissociation of the acidic functional groups.

Furthermore, titration of biomass with a base leads to the opening of its dense cell wall structure which may change the spatial disposition of functional groups and lead to the titration of sites normally inaccessible. This phenomenon results in a titration hysteresis generally observed when titrating backward organic complex compounds (Claessens and Behrends, 2004; Sposito, 1984). The same configuration changes concerning the expansion of fulvic acids macromolecules with an increase in pH of the titration medium were observed causing the buffering effect of the dissociation of the carboxylic groups extending over a wide pH range (Sposito and Holtzclaw, 1977).

An electrostatic function W (Tanford, 1961) could be introduced to take into account the different restrictions mentioned above, in dissociation of acidic groups due to their proximity and changes in configuration during a basic titration and to differentiate between pK_{app}, calculated constant in the present work and pK_{INT}, the intrinsic pK at zero degree of dissociation. Omitting the electrostatic effect due to the charge density and the configuration changes, the ionization constants K_a calculated in the present work are considered as apparent constants and not intrinsic.

4.2.2. Infrared analysis

The same organic functional groups and wave numbers were identified in the different types of biomass selected for the present work. These groups compare with those identified in other studies addressing infrared spectra of biomass (Heber et al., 1952) or proteins (Gendreau et al., 1982). Infrared (IR) spectra of these organic materials showed the presence of amine $R\text{-}NH_2$ (amino acids, proteins, glycoproteins, etc.), carboxylic acids (fatty acids, lipopolysaccharides, etc.) and phosphates. The characteristic absorption bands of hydroxyl and amine groups were identified at 3425 and $3300\,cm^{-1}$, alkyl chains at $2925–2800\,cm^{-1}$, $C{=}O$ of the protonated carboxylic groups or esters groups at $1740\,cm^{-1}$, $C{=}O$ of the carboxylic groups of aminoacids at $1710\,cm^{-1}$, amide and phosphate groups appeared at $1640\,cm^{-1}$ and between 1150 and $1030\,cm^{-1}$, respectively. The wave numbers at 1075 and at $726\,cm^{-1}$ were attributed to the P–O vibration of the $(C\text{-}PO_3^{2-})$ moiety and to the S–O link of the $(C\text{-}SO_3^-)$ groups, respectively. The IR of $T.\ ferrooxidans$ biomass indicated the presence of the sulfate group bands $(1205–1156–620–590\,cm^{-1})$.

As an example, the relevant infrared wave numbers for $R.\ arrhizus$ biomass are listed in Table 2. The infrared vibrations indicated the presence of protonated carboxylic, amine and phosphate groups confirming the acid–base titration results.

4.3. pH influence on lead sorption

Potentiometric titration is used to estimate the quantity of the free and/or protonated sites, to define precisely the optimal sorption capacity at a given pH value and to establish the optimum condition of biomass surfaces (choice of the pH value) for metal sorption by $R.\ arrhizus$ and $C.\ glutamicum$.

However, one must notice that the total organic acidity value depends on the solution pH value. Consequently, during a metal uptake experiment, the amount of sorbed metal should be compared to the A_{TO} expressed at the studied pH and not to the A_{TO} calculated after base titration of the biomass

Table 2

Characteristic infrared absorption frequencies of $R.\ arrhizus$ biomass

Wave number (cm^{-1})	Band assignment
3425	Hydroxyl OH of water
3300	Amine groups
2925–2800	Alkyl chains (CH_3 and CH_2 sym. and asym. stretch)
1740	$>C{=}O$ stretch, protonated carboxylic groups, esters groups or fatty acids
1710	$>C{=}O$ stretch, carboxylic groups of aminoacids or esters
1640	Amide groups, $(C{=}O)$ different conformations
1544 and 1418	C–O bend from carboxylate ions
1300	Amide II (C–N), $S{=}O$ of the sulfonates groups, COO^- groups of the fatty acids
1150–1030	P–O–C links of the organic phosphated groups
1075	P–O of the $(C\text{-}PO_3^{2-})$ moiety
726	S–O link of the $(C\text{-}SO_3^-)$ groups

(pH = 10.5). The calculation of the A_{TO} for a specific pH value was based on the progressive ionization reactions and on their dissociation coefficients α illustrated in Fig. 4.

After the base titration conducted in the present work, results showed that $R.\ arrhizus$ biomass had a total organic acidity, at pH 10.5, 2 times higher than that of $C.\ glutamicum$ (Table 1). At pH 6, the two biomass types, $R.\ arrhizus$ and $C.\ glutamicum$, exhibited $0.75\,me\,g^{-1}$ (30%) and $0.73\,me\,g^{-1}$ (56%) of the total number of acidic active sites, respectively (Table 3).

Knowing that carboxylic sites are mostly involved in the heavy metal biosorption by biomass (Sarret et al., 1998; Volesky, 2003), the pH preferred for sorption uptake should be between $pK_a \pm 1$. For example, sorption of lead by $C.\ glutamicum$ and $R.\ arrhizus$ biomass indicates an optimum pH of 6. It appears that 64% ($Pb_{(uptake)} = 0.48\,me\,g^{-1}$) and 38% ($Pb_{(uptake)} = 0.28\,me\,g^{-1}$) of A_{TO} were involved during lead sorption by $R.\ arrhizus$ and $C.\ glutamicum$, respectively (Table 3).

The pH influence can be explained by different affinity values depending on the nature of cations (protons, lead) and their properties: electronegativity, ionic radius, state of the surface, steric configuration, etc. Consequently, the solution pH affects the sorption of cations that compete with protons for sorption on the active sites. At pH 4, the available sites on the surface of the biomass are protonated and the calculated A_{TO} at pH 4 using Gran's method were very low (Table 3), hence sorption of cations is more difficult.

Table 3
Comparison of the values of A_{TO} (total organic acidity) and the lead uptake (me g^{-1}) at pH 4, 5, 6 of *C. glutamicum* and *R. arrhizus*. Calculation of the occupied sites (% of A_{TO})

pH	*C. glutamicum*			*R. arrhizus*		
	A_{TO} (me g^{-1})	Pb uptake (me g^{-1})	Occupied sites (%)	A_{TO} (me g^{-1})	Pb uptake (me g^{-1})	Occupied sites (%)
4	0.32	0.11	34	0.38	0.14	37
5	0.54	0.20	37	0.58	0.35	60
6	0.73	0.28	38	0.75	0.48	64

The understanding of the nature of charged functional groups in the cell walls of fungi and bacteria is necessary to improve and explain different industrial processes involving biosorption and adhesion. Biosorption is capable of cost-effectively removing heavy metals from polluted waters (Figueira et al., 1996; Guibal and Roulph, 1990; Kratochvil and Volesky, 1998). Two components are involved in such sorption reactions, specific functional groups of the biomass, such as carboxylic groups, and the metal ion.

The high-resolution potentiometric titration using Gran's method represents a novel approach to studying the proton dissociation from an organic heterogeneous solid and to evaluating three types of ion exchanging sites based on the existence of three mean types of acidic functional groups. The knowledge of the distribution of acidities and their different pK_a values is important for evaluating the effect of pH on the sorption process performance and for estimating the quantity of the reactive sites, at the given pH, available for important binding reactions.

References

Beveridge, T.G., 1986. The immobilization of soluble metals by bacterial walls. Biotechnol. Bioeng. Symp. 16, 127–140.

Brunelot, G., Adrian, P., Rouiller, J., Guillet, B., Andreux, F., 1989. Determination of dissociable acid groups of organic compounds extracted from soils, using automated potentiometric titration. Chemosphere 19 (8/9), 1413–1419.

Claessens, J., Behrends, T.P.V.C., 2004. What do acid–base titrations of live bacteria tell us? A preliminary assessment. Aquatic Sci. 66, 19–26.

Coleman, N.T., Weed, S.B., McCraken, R.J., 1959. Cation exchange capacity and exchangeable cations in Piedmont soils of North Carolina. Soil Sci. Soc. Am. Proc. 23, 146–149.

Cox, J.S., Smith, D.S., Warren, L.A., Ferris, F.G., 1999. Characterizing heterogeneous bacterial surface functional groups using discrete affinity spectra for proton binding. Environ. Sci. Technol. 33, 4514–4521.

Daughney, C.J., Fowle, D.A., Fortin, D., 2001. The effect of growth phase on proton and metal adsorption by *Bacillus subtilis*. Geochim. Cosmochim. Acta 65, 1025–1035.

de Wit, J.C.M., Van Riemsdijk, W.H., Koopal, L.K., 1993. Proton binding to humic substances. I. Electrostatic effects. Environ. Sci. Technol. 27, 2005–2014.

Figueira, M.M., Volesky, B., Ciminelli, V.S.T., 1996. Assessment of interference in biosorption of a heavy metal. Biotechnol. Bioeng. 54 (4), 344–350.

Fourest, E., Volesky, B., 1996. Contribution of sulfonate groups and alginate to heavy metal biosorption by the dry biomass of *Sargassum fluitans*. Environ. Sci. Technol. 30, 277–282.

Fourest, E., Canal, C., Roux, J.C., 1994. Improvement of heavy metal biosorption by mycelial dead biomasses (*Rhizopus arrhizus*, *Mucor miehei* and *Penicillium chrysogenum*): pH control and cationic activation. FEMS Microbiol. Rev. 14, 325–332.

Gadd, G.M., 1988. Accumulation of metals by microorganisms and algae. Biotechnology 401–433.

Gendreau, R.M., Leininger, R.I., Winters, S., Jacobsen, R., 1982. Fourier transform infrared spectroscopy for protein–surface interactions. Biomaterials 1, 371–393.

Gran, G., 1952. Determination of the equivalence point in potentiometric titrations. Part II. Analyst 77, 661–671.

Guibal, E., Roulph, C., 1990. Uranium sorption by fungi: application to treatment of low charge effluents. J. Français d'Hydrol. 21 (2), 229–240.

Heber, J.R., Stevenson, R., Boldman, O., 1952. Infrared spectroscopy as a means for identification of bacteria. Science 116, 111–112.

Kratochvil, D., Volesky, B., 1998. Advances in the biosorption of heavy metals. Trends Biotechnol. 16, 291–300.

Kucharkowski, R., Kluge, W., Kasper, E., Drescher, A., 1984. A system for automatic titrations with computer interpretation of data. Proceedings of the Fourth Symposium on Ion-Selective Electrodes, pp. 533–538.

Martell, A.E., Smith, R.M., 1974. Critical Stability Constants, 1–6 ed. Plenum Press, New York.

McBride, M.B., 1994. Environmental Chemistry of Soils. Oxford University Press, New York, 416pp.

Mukai, T., Takimoto, K., Kohno, T., Okada, M., 2000. Ultrafiltration behaviour of extracellular and metabolic

products in activated sludge system with UF separation process. Water Res. 34, 902–908.

Pagnanelli, F., Veglio, F., Toro, L., 2004. Modelling of the acid–base properties of natural and synthetic adsorbent materials used for heavy metal removal from aqueous solutions. Chemosphere 54, 905–915.

Rossotti, F.J.C., Rossotti, H., 1965. Potentiometric titrations using Gran Plots. J. Chem. Educ. 42 (7), 375–378.

Roux, J.C., Lhomme, B., De Vôgue, B., Neyton, J., Teisador, J.P., 1988. *Rhizopus arrhizus* culture and biosorption of heavy metals in fluidised bed columns. Soc. Française Microbiol. 233–243.

Sarret, G., Manceau, A., Spadini, L., Roux, J.C., Hazemann, J.L., Soldo, Y., Eybert-Berard, L., Menthonnex, J.J., 1998. Structural determination of Zn and Pb binding sites in *Penicillium chrysogenum* cell walls by EXAFS Spectroscopy. Environ. Sci. Technol. 32, 1648–1655.

Schiewer, S., Volesky, B., 1997. Ionic strength and electrostatic effects in biosorption of protons. Environ. Sci. Technol. 31, 1863–1871.

Sing, C., Yu, J., 1998. Copper adsorption and removal from water by living mycelium of white-rot fungus *Phanerochaete chrysosporium*. Water Res. 32 (9), 2746–2752.

Sposito, G., 1984. The Surface Chemistry of Soils. Oxford University Press, New York, 234pp.

Sposito, G., Holtzclaw, K.M., 1977. Titration studies on the polynuclear, polyacidic nature of fulvic acid extracted from sewage sludge soil mixtures. Soil Sci. Soc. Am. J. 3 (41), 330–336.

Stumm, W., 1992. Chemistry of the Solid–Water Interface. Wiley, New York, 448pp.

Tanford, C., 1961. Physical Chemistry of Macromolecules. Wiley, New York, 710pp.

Temple, K.L., Colmer, A.R., 1951. The autotrophic oxidation of iron by a new bacterium *Thiobacillus ferrooxidans*. J. Bacteriol. 62, 605–611.

Texier, A.C., Andres, Y., Illemassene, M., Le Cloirec, P., 2000. Characterization of lanthanide ions binding sites in the cell wall of *Pseudomonas aeruginosa*. Environ. Sci. Technol. 34, 610–615.

Volesky, B., 2003. Sorption and Biosorption, BV Sorbex, Inc., Canada, 316pp.

Volesky, B., May, H., Holan, Z.R., 1993. Cadmium biosorption by *Saccharomyces cerevisiae*. Biotechnol. Bioeng. 41, 826–829.

Yee, N., Fein, J., 2001. Cd adsorption onto bacterial surfaces: a universal adsorption edge? Geochim. Cosmochim. Acta 65, 2037–2042.

Young, S.D., Bache, B.W., Welch, D., Anderson, H.A., 1981. Analysis of potentiometric titration of natural and synthetic polycarboxylate. J. Soil Sci. 32, 579–592.